Demixing Instability in Polymer Blends Undergoing Polycondensation Reactions

P. I. C. Teixeira,* D. J. Read, and T. C. B. McLeish

IRC in Polymer Science and Technology, Department of Physics, University of Leeds, Leeds LS2 9JT, United Kingdom

Received June 16, 1999; Revised Manuscript Received February 22, 2000

ABSTRACT: The stability with respect to demixing of a reacting binary polymer blend is investigated. In the spirit of earlier work (Read, D. J. *Macromolecules* **1998**, *31*, 899), we combine the random phase approximation for the free energy with a Markov chain model for the chemistry to obtain the spinodal as a function of the relevant degrees of reaction. These are then calculated by assuming a simple second-order chemical kinetics. Results are presented, for both linear and branched systems, which illustrate the effects of varying the reaction rates and/or the stiffnesses of the constituent polymer "building blocks". Phenomena arise that are not captured by theories assuming equality of these parameters.

1. Introduction

Many industrially produced polymeric materials exhibit microphase-separated structures. Examples are high-impact polystyrene, or HIPS, widely used in pharmaceutical packaging,[1] and polymer-dispersed liquid crystals (PDLCs), which show promise for display device applications.[2] In both systems, the mesoscale morphology determines the properties of practical interest: elastic and rheological in the former and electrooptical in the latter.

This demixing of an initially homogeneous blend can be driven by a sudden temperature change (thermally induced phase separation, or TIPS) or by the increase in length of the molecules during polymerization (polymerization-induced phase separation, or PIPS).[3] In the latter case, it can occur at moderate conversion, for which the polymer chains are still fairly short.[4,5] Thus the chemistry provides additional degrees of freedom, and by manipulating it we have access to a richer variety of structures than by varying the temperature alone.

If the building blocks are such that they can and do associate in a large number of different irregular sequences, one speaks of random multiblock copolymers. These find applications as adhesives, compatibilizers, emulsifiers, and elastomers. From a more fundamental point of view, they are objects with quenched disorder, and, as pointed out by de Gennes,[6] their phase behavior will depend not only on chemical composition but also on the correlations between blocks. In particular, de Gennes predicted that, as the randomness in the distribution of block lengths increases, the wave vector at which the disordered (mixed) phase becomes unstable should vanish at a Lifshitz point, signaling a crossover from copolymer-like (microphase separation) to homopolymer-like (bulk phase separation) behavior. Indeed, mean-field (MF) calculations have shown that the uniform phase of a copolymer composed of two types of monomer with a tendency to alternate first becomes unstable with respect to a spatially inhomogeneous mesophase.[7,8] By contrast, bulk phase separation into two homogeneous phases is favored by "ideally random",[9] copolymers (where the identities of consecutive monomers are not correlated) or "blocky" copolymers (containing long sequences of monomers of the same type). These works highlight the importance of molecular architecture in determining the thermodynamics of a melt.

How realistic the MF picture is is a matter of much debate. One early conjecture was that the MF third-order ordering transition of ideally random copolymers[9−11] is preempted by the formation of a glassy state;[12,13] later the same transition was found to be suppressed[14] or driven first-order[15−20] by fluctuations, which may also destroy the Lifshitz point and bulk phase separation at high polydispersity.[21] By contrast, there appears to be a consensus that *correlated* random multiblock copolymers can microphase-separate:[22] The full phase diagram has been worked out in the limit of weak randomness, both neglecting[22,23] and including[24−27] fluctuations, and a very general Landau free energy derived.[28] No bulk instability occurs in the limit of infinitely long polymers,[27] but it is still possible if the molecules are relatively short.[7,8] Finally, Semenov[29] and Semenov and Likhtman[30] have revealed the very subtle role of polydispersity in these systems: within MF theory and in the long-molecule limit where fluctuations are negligible, secondary domains characterized by an internal primary microstructure are predicted to form near the transition lines between different primary morphologies.

Traditionally, one investigates phase stability by looking at the convexity of the free energy, i.e., by locating the spinodal. Hence we require a theory that will give us the free energy of a reacting polymer blend to at least second order in the (total) density, as a function not only of the temperature and parameters characterizing the microscopic interactions of the system (typically the Flory χ parameter) but also of the relevant degrees of reaction, i.e., the conversions of the chemically active components. To this end we generalize an earlier model by one of us,[31] who applied the random phase approximation (RPA)[32,33] to a Markov chain system.[34] The latter is a mathematical description of a polymerization process that gives an expression for the probability distribution of monomers along each chain. In ref 31 it was assumed that the reaction rates of all

* Author for correspondence.

10.1021/ma990954d CCC: $19.00
Published on Web 04/29/2000

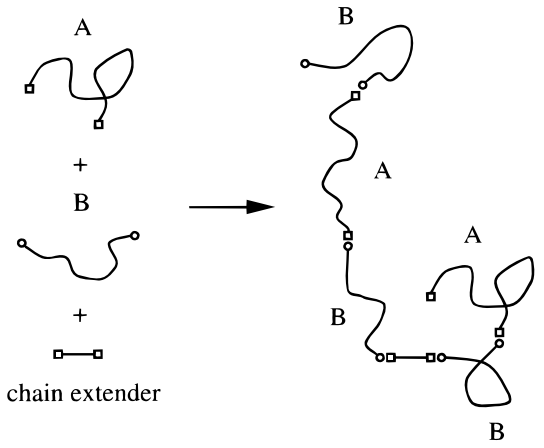

Figure 1. Schematics of the polycondensation reaction under study. ○ end groups on B blocks react with □ groups on A blocks or on chain extenders to form random multiblock copolymers. The latter are polydisperse in length and may be more or less miscible than the original unconnected blocks.

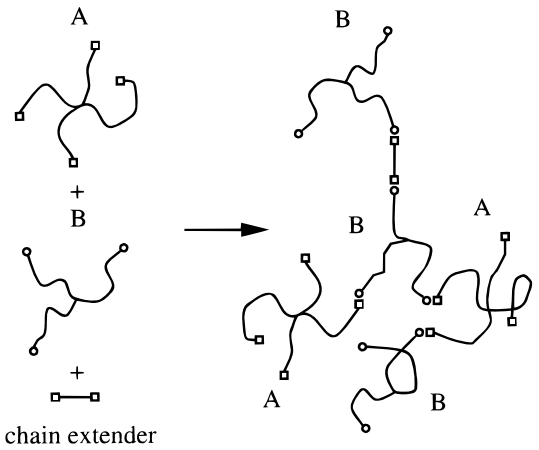

Figure 2. Same as Figure 1, but where the building blocks are multiarm star polymers and we have chosen $m_A = 4$, $m_B = 3$ for definiteness.

reactive groups in the system were identical and that blocks A and B had the same stiffness (as measured by their Kuhn lengths). Here we remove both these approximations, for a more realistic description.

In particular, we are concerned with blends undergoing polycondensation reactions of the type illustrated schematically in Figure 1, which is representative of many situations of practical interest. There are two types of "building blocks", A and B, each of which is itself a (sometimes short) polymer. A has two reactive end groups of type □, and B two reactive end groups of type ○. A □ group can only react with a ○ group, and therefore an A block cannot attach itself to another A block. However, it is useful to allow B blocks to follow one another without an intervening A block: for this purpose we include a third component that we call "chain extender", a shorter molecule with end groups of type □. The role of the chain extender is to give us more control over the molecular architecture: for low extender content the polymers will consist mostly of alternating A and B blocks and thus be more like diblock copolymers, whereas higher extender content will favor *variable-length* sequences of B blocks and hence a more (polydisperse) "homopolymer-like" behavior. We assume that the chain extender is much shorter than the A or B blocks and that its interactions with either of these do not significantly affect phase stability, so that we can treat the initial system as a binary mixture of A's and B's. The end result will be a polydisperse blend of random multiblock copolymers. Because these are correlated[27] and not very long,[7,8] we expect to see both micro and bulk phase separation. Furthermore, we shall explore the consequences of a more general architecture, by allowing A and B to be star polymers with an arbitrary number of arms (see Figure 2).

This paper is organized as follows: in section 2.1 we briefly summarize the RPA formalism and quote the expression for the spinodal. Then in sections 2.2 (linear blocks) and 2.3 (multiarm star blocks) we generalize the Markov chain model to the case of two different reaction rates and Kuhn lengths and derive the corresponding analytic expression for the structure factor of reacting incompressible blends in terms of the degrees of completion of the two reactions. It is shown in section 2.4 how these can be obtained from a simple model for the chemical kinetics. In section 3 we present our results for the effect of different block stiffnesses and chemical reaction rates on the spinodal and wave vector of first instability. Finally, some conclusions and directions for future work are collected in section 4.

2. Theory

2.1. Stability of a Binary Fluid Mixture. In this subsection we just summarize the basic results of the RPA and refer the reader to refs 31−33 for details. For simplicity, consider an incompressible blend of A and B blocks, of total density ρ, contained in a volume Ω. (As said above we shall neglect the chain extender, which as a small molecule plays little role in the phase separation.) Let $\rho^A(\mathbf{r})$ be the density of A *monomers* (i.e., the constituents of A blocks) at point $\mathbf{r}$

$$\rho^A(\mathbf{r}) = \sum_{\alpha,l} y_l^\alpha \delta(\mathbf{r} - \mathbf{r}_l^\alpha) \tag{1}$$

with Fourier transform

$$\rho_{\mathbf{q}}^A = \int_\Omega \exp(i\mathbf{q}\cdot\mathbf{r})\rho^A(\mathbf{r})\, d\mathbf{r} = \sum_{\alpha,l} y_l^\alpha \exp(i\mathbf{q}\cdot\mathbf{r}_l^\alpha) \tag{2}$$

where $\mathbf{r}_l^\alpha$ is the position of the lth monomer on chain α and $y_l^\alpha = 1(0)$ if that monomer is part of an A (B) block. (A *chain* is a sequence of blocks.) Likewise the density of B monomers is

$$\rho_{\mathbf{q}}^B = \sum_{\alpha,l} (1 - y_l^\alpha) \exp(i\mathbf{q}\cdot\mathbf{r}_l^\alpha) \tag{3}$$

The main result of the RPA for an incompressible blend ($\rho_{\mathbf{q}}^A + \rho_{\mathbf{q}}^B = \rho\delta(\mathbf{q})$) is the expression for the scattering structure factor

$$S(\mathbf{q}) = \frac{v_0}{\Omega}\langle \rho_{\mathbf{q}}^A \rho_{-\mathbf{q}}^A \rangle = \left[\frac{1}{S_{non}(\mathbf{q})} - 2\chi\right]^{-1} \tag{4}$$

where $\langle ... \rangle$ denotes an average over conformations of the *interacting* chains, v_0 is the volume of an individual A or B monomer, χ is the Flory interaction parameter, and $S_{non}(\mathbf{q})$ is the structure factor of the noninteracting system, given by

$$S_{non}(\mathbf{q}) = \frac{s_0^{AA} s_0^{BB} - (s_0^{AB})^2}{s_0^{AA} + s_0^{BB} + 2s_0^{AB}} \tag{5}$$

with s_0^{AA}, s_0^{BB}, and s_0^{AB} the structure factors of the components of the blend in the noninteracting limit

$$s_0^{AA} = \frac{v_0}{\Omega}\langle \rho_{\mathbf{q}}^{A}\rho_{-\mathbf{q}}^{A}\rangle_0 \tag{6}$$

$$s_0^{AB} = \frac{v_0}{\Omega}\langle \rho_{\mathbf{q}}^{A}\rho_{-\mathbf{q}}^{B}\rangle_0 \tag{7}$$

$$s_0^{BB} = \frac{v_0}{\Omega}\langle \rho_{\mathbf{q}}^{B}\rho_{-\mathbf{q}}^{B}\rangle_0 \tag{8}$$

$\langle ... \rangle_0$ now being an average over configurations of *noninteracting* chains. Although it may appear unnatural to assume A and B monomers to possess the same volume, we are free to (re)define "monomer" in a way that satisfies this, without loss of generality. For example, suppose a polymer of species α contains N_α^{chem} chemical repeat units, each of volume v_α^{chem}. Then the "renormalized" polymer will consist of N_α repeat units, each of volume v_0, where

$$N_\alpha = \frac{v_\alpha^{chem} N_\alpha^{chem}}{v_0} \tag{9}$$

with an appropriate redefinition of the monomer step length. In this connection, it is important to realize that values for the Flory χ parameter are frequently quoted with respect to an (arbitrary) reference volume that bears no relation to actual chemical monomers; in all such cases, the above renormalization is implied.

Within the RPA, the free energy is

$$F[\{\rho_{\mathbf{q}}^{A}\}] = \frac{\Omega}{2}\sum_{\mathbf{q}} S^{-1}(\mathbf{q})\rho_{\mathbf{q}}^{A}\rho_{-\mathbf{q}}^{A} \tag{10}$$

with $S(\mathbf{q})$ given by eq 4 with eq 5. (Note that it is implicit in the above that the interaction between monomers is short-ranged; otherwise, we would have $\chi \equiv \chi(\mathbf{q})$.) The spinodal is reached when $S(\mathbf{q})$ diverges at some wavenumber $\mathbf{q} = \mathbf{q}^*$. From eq 4 this occurs when $S_{non}(\mathbf{q})$ is maximum, whence the critical—spinodal—value of χ is

$$\chi_S = \frac{1}{2\ \max_{\mathbf{q}}[S_{non}(\mathbf{q})]} \tag{11}$$

It is now clear that the nature of the spinodal instability is determined by the value of $\mathbf{q}^*$: $\mathbf{q} = 0$ corresponds to the growth of long-range fluctuations and thus bulk phase separation, whereas a finite $\mathbf{q}^*$ means demixing on a microscopic scale.

In order to proceed we require expressions for s_0^{AA}, s_0^{AB}, and s_0^{BB} entering eq 5. For the system under investigation, which is undergoing a chemical reaction, these are obtained from the Markov chain model in the following subsection.

2.2. The Generalized Markov Chain Model. Again we merely sketch the details of the derivation and refer readers to ref 31 for details. The Markov chain model assumes that monomers are added to each chain in random fashion and that the probability of attachment of any block to an end of a preexisting chain depends only on the identities of the two blocks reacting but not on the previous "history" of the chain. Thus the key object is the probability matrix P, defined as

$$\boldsymbol{P} = \begin{pmatrix} p_{AA} & p_{AB} \\ p_{BA} & p_{BB} \end{pmatrix} \tag{12}$$

where $p_{\alpha\beta}$ is the probability that a block of type α follows one of type β. This, together with the matrix of propagators

$$\boldsymbol{G} = \begin{pmatrix} G_A & 0 \\ 0 & G_B \end{pmatrix} \tag{13}$$

enables us to write the structure factors for the noninteracting blend as

$$s_0^{AA} = \frac{n_A v_0}{\Omega}\left[J_A + 2H_A^2 \begin{pmatrix}1 & 0\end{pmatrix}\boldsymbol{P}\cdot(\boldsymbol{I} - \boldsymbol{G}\cdot\boldsymbol{P})^{-1}\begin{pmatrix}1\\0\end{pmatrix}\right] \tag{14}$$

$$s_0^{AB} = \frac{n_A v_0}{\Omega}\left[2H_A H_B \begin{pmatrix}0 & 1\end{pmatrix}\boldsymbol{P}\cdot(\boldsymbol{I} - \boldsymbol{G}\cdot\boldsymbol{P})^{-1}\begin{pmatrix}1\\0\end{pmatrix}\right] \tag{15}$$

$$s_0^{BB} = \frac{n_B v_0}{\Omega}\left[J_B + 2H_B^2 \begin{pmatrix}0 & 1\end{pmatrix}\boldsymbol{P}\cdot(\boldsymbol{I} - \boldsymbol{G}\cdot\boldsymbol{P})^{-1}\begin{pmatrix}0\\1\end{pmatrix}\right] \tag{16}$$

where n_A (n_B) is the number of A (B) blocks in volume Ω, $\boldsymbol{I}$ is the identity matrix, and J_A (J_B) and H_A (H_B) are, respectively, the "self-term" and "coterm" of an A (B) block.[31] G_α, J_α, and H_α are functions of the wave vector $q = |\mathbf{q}|$ and the nature of the block: in what follows we shall take them to be Gaussian coils, characterized by a degree of polymerization N_α and a Kuhn length b_α (here α = A, B). N_α is *defined* as the number of α monomers, of volume v_0 each, in an α block; if $R_{g,\alpha}$ is the (experimentally measurable) radius of gyration of such a block, then $b_\alpha = R_{g,\alpha}(6/N_\alpha)^{1/2}$. Note that the above definition of a monomer unit, which we have found particularly convenient to adopt, is *not* related to the persistence length; instead, the chain stiffness, introduced via the Kuhn length, is absorbed into the radius of gyration. Analytical expressions for the propagator, coterm, and self-term of a Gaussian coil have been derived in ref 31 and are quoted below as eqs 25−29.

At this stage it is useful to define a few new quantities. The *number fraction of blocks of type* A (referred to the total number of A and B blocks *only*) is

$$f_A = \frac{n_A}{n_A + n_B} \tag{17}$$

while the *volume fraction of* A *monomers* (assuming all monomers have the same volume v_0) is

$$\phi_A = \frac{n_A N_A}{n_A N_A + n_B N_B} \tag{18}$$

and the *mean* ("number average") *block size* is

$$N = f_A N_A + f_B N_B \tag{19}$$

The three parameters f_A (with $f_B = 1 - f_A$), ϕ_A (with $\phi_B = 1 - \phi_A$), and N (or N_A, or N_B) suffice to specify the system completely at the start of the reaction. Indeed, it is easy to show, e.g., that

$$N_B = N_A \frac{\frac{1}{\phi_A} - 1}{\frac{1}{f_A} - 1} \tag{20}$$

Crucially, in order that the assumption of Gaussian behavior be valid, we must have $N_A \gg 1$ *and* $N_B \gg 1$.

It remains to find the elements of $\boldsymbol{P}$: these are determined by the chemistry (see Figure 1). We consider only the case of a stoichiometric blend, where there are no unreacted groups left at the end; this fixes the number of extender blocks to be $n_e = n_B - n_A$ (and $f_e = f_B - f_A$). Because an A block cannot follow another, $p_{AA} = 0$. On the other hand, an A block can only be followed by a B block; this happens with a probability p_A, which equals the degree of reaction of A blocks, yielding $p_{BA} = p_A$ (see Figure 3). The remaining matrix elements are a little harder: a B block can react with an A block or with a chain extender. The probability that an A block follows (has reacted with) a B block will be the number of reacted A blocks, $n_A p_A$, divided by the total number of B blocks, n_B; hence, $p_{AB} = (n_A/n_B)p_A = (f_A/f_B)p_A$. Finally, the probability that a B block follows another B block equals the probability that a chain extender reacts with a B chain end times the probability that that extender is then followed by a B block. The latter is just p_e, the probability that an extender block has reacted. Now, the number of reacted extender blocks will be $n_e p_e$. By the same reasoning as above, the probability that this reaction occurred is $(n_e/n_B)p_e = (1 - f_A/f_B)p_e$, where we have used the fact that the blend is stoichiometric. In summary

$$\boldsymbol{P} = \begin{pmatrix} 0 & \left(\frac{f_A}{f_B}\right)p_A \\ p_A & \left(1 - \frac{f_A}{f_B}\right)p_e^2 \end{pmatrix} \tag{21}$$

Inserting $\boldsymbol{P}$ from eq 21 into eqs 14−16 we finally obtain

$$s_0^{AA} = N\left(\frac{\phi_A^2}{f_A}\right)\left[j_A + \frac{2h_A^2 G_B p_A^2 f_A}{1 - f_A - p_e^2 G_B(1 - 2f_A) - p_A^2 G_A G_B f_A}\right] \tag{22}$$

$$s_0^{AB} = N(\phi_A\phi_B)\left[\frac{2h_A h_B p_A}{1 - f_A - p_e^2 G_B(1 - 2f_A) - p_A^2 G_A G_B f_A}\right] \tag{23}$$

$$s_0^{BB} = N\left(\frac{\phi_B^2}{f_B}\right)\left\{j_B + \frac{2h_B^2[G_A p_A^2 f_A + (1 - 2f_A)p_e^2]}{1 - f_A - p_e^2 G_B(1 - 2f_A) - p_A^2 G_A G_B f_A}\right\} \tag{24}$$

where the propagator, coterm, and self-term of a Gaussian block are given by[31]

$$G_\alpha = \exp(-Q_\alpha^2) \tag{25}$$

$$H_\alpha = N_\alpha h_\alpha(Q_\alpha^2) \tag{26}$$

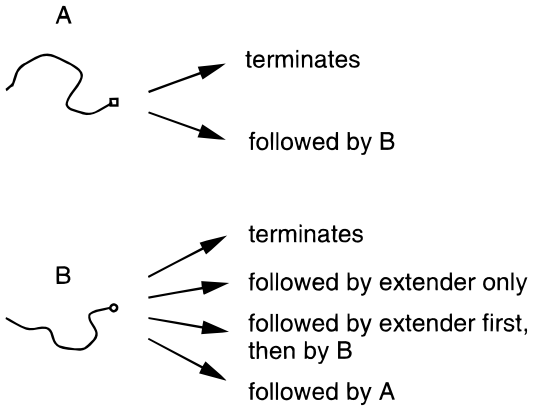

Figure 3. Possible arrangements that may follow an A or a B block in the reaction process.

$$J_\alpha = N_\alpha^2 j_\alpha(Q_\alpha^2) \tag{27}$$

with $Q_\alpha^2 = q^2 b_\alpha^2 N_\alpha/6 \equiv q^2 R_{g,\alpha}^2$ and

$$h_\alpha(x) = \frac{1}{x}(1 - e^{-x}) \tag{28}$$

$$j_\alpha(x) = \frac{2}{x^2}(e^{-x} - 1 + x) \tag{29}$$

Note that the structure factor, and therefore the spinodal, will be a function of time through its dependence on the degrees of reaction.

2.3. Extension to Branched Systems. The formalism summarized in the preceding section lends itself to a number of generalizations. Perhaps the simplest is to consider different types of building blocks: propagators, coterms, and self-terms have been calculated for rods[35] and for star polymers.[31] In view of the practical and conceptual importance of branched molecular architectures (see, e.g., ref 36 and references therein), we focus here on a reacting blend of m_A-branched A blocks and m_B-branched B blocks (see Figure 2, where $m_A = 4$ and $m_B = 3$), for which a number of results already exist.[31]

It is convenient to introduce the new variable "valence fraction of A", η_A, defined as the ratio of the number of reactive (□) groups on the A blocks to the total number of reactive groups (□ and ○) on A and B blocks:

$$\eta_A = \frac{m_A n_A}{m_A n_A + m_B n_B} \tag{30}$$

It follows from our assumption of stoichiometry (now $m_A n_A - m_B n_B = 2n_e$; see section 2.4) that $0 < \eta_A < 1/2$, whereas the range of f_A depends on m_A. Thus fixing η_A while varying m_A or m_B ensures a constant average number of B blocks between A blocks in the final reacted product. Similarly, one defines $\eta_B = 1 - \eta_A$. η_A is related to f_A via

$$f_A = \frac{m_B \eta_A}{m_B \eta_A + m_A \eta_B} \tag{31}$$

From ref 31 the propagator, coterm, and self-term of an m_α-branched block are

$$G_\alpha^* = (m_\alpha - 1)(G_{arm}^\alpha)^2 \tag{32}$$

$$H^*_\alpha = N_\alpha h^*_A = \frac{N_\alpha}{m_\alpha}[1 + (m_\alpha - 1)G^\alpha_{arm}]h^\alpha_{arm} \quad (33)$$

$$J^*_\alpha = N^2_\alpha h^*_A = \frac{N^2_\alpha}{m_\alpha}[j^\alpha_{arm} + (m_\alpha - 1)(h^\alpha_{arm})^2] \quad (34)$$

where the $*$ superscript denotes "star" polymers and

$$G^\alpha_{arm} = \exp\left(-\frac{Q^2_\alpha}{m_\alpha}\right) \quad (35)$$

$$h^\alpha_{arm} = h_\alpha\left(\frac{Q^2_\alpha}{m_\alpha}\right) \quad (36)$$

$$j^\alpha_{arm} = j_\alpha\left(\frac{Q^2_\alpha}{m_\alpha}\right) \quad (37)$$

are the corresponding quantities associated with each arm of a star, with $h_\alpha(x)$, $j_\alpha(x)$ given by eqs 28 and 29, respectively. Working through eqs 14−16, we obtain the structure factors for the stoichiometric noninteracting blend of A and B blocks of arbitrary functionality:

$$s^{AA}_0 = N\left(\frac{\phi^2_A}{f_A}\right)\left[j^*_a + \frac{m_A(h^*_A)^2 G^*_B p^2_A \eta_A}{1 - \eta_A - p^2_e G^*_B(1 - 2\eta_A) - p^2_A G^*_A G^*_B \eta_A}\right] \quad (38)$$

$$s^{AB}_0 = N(\phi_A\phi_B)\left(\frac{m_A m_B}{m_A f_A + m_A f_B}\right) \times \left[\frac{h^*_A h^*_B p_A}{1 - \eta_A - p^2_e G^*_B(1 - 2\eta_A) - p^2_A G^*_A G^*_B \eta_A}\right] \quad (39)$$

$$s^{BB}_0 = N\left(\frac{\phi^2_B}{f_B}\right)\left\{j^*_B + \frac{m_B(h^*_B)^2[G^*_A p^2_A \eta_A + (1 - 2\eta_A)p^2_e]}{1 - \eta_A - p^2_e G^*_B(1 - 2\eta_A) - p^2_A G^*_A G^*_B \eta_A}\right\} \quad (40)$$

In the limit of linear chains, $m_A = m_B = 2$, $\eta_A = f_A$, and eqs 22−24 are recovered.

Specific to branched blocks is the mathematical breakdown of the theory at the percolation threshold, corresponding to the vanishing of the denominator in eqs 38−40 for $\mathbf{q} = \mathbf{0}$, i.e.,

$$(m_A - 1)\eta_A p^2_A + (1 - 2\eta_A)p^2_e = \frac{1 - \eta_A}{m_B - 1} \quad (41)$$

Note, however, that this divergence cancels out in eq 5 and consequently the spinodal is not affected, reflecting the fact that it measures the loss of *local* stability of the mixed state. Finally, one actually expects that the theory will break down earlier than eq 41 suggests, in fact when a significant number of loops, neglected in the present treatment, appear. de Gennes[37] calculated the size of the Ginzburg region around the gel point occurring at $p = p_c$, where $p \equiv p_B$ is the degree of reaction of species B, to be

$$\Delta p \equiv p_c - p \sim N^{-1/3} \quad (42)$$

Within this region percolation statistics are expected to dominate. Consequently, our theory is only applicable for $p_c \gg N^{-1/3}$, i.e., to sufficiently long blocks that are not too heavily branched.

2.4. Chemical Kinetics. We thus require the probabilities that a □ group on an A block or on an extender block has reacted, which are the same as the respective *degrees of reaction*. These can be obtained from the rate equations for the three chemical reactions; see Figure 1

$$\frac{dx_{\square A}}{dt} = -\kappa x_{\square A} x_{\bigcirc B} \quad (43)$$

$$\frac{dx_{\bigcirc B}}{dt} = -\kappa x_{\square A} x_{\bigcirc B} - \kappa' x_{\square e} x_{\bigcirc B} \quad (44)$$

$$\frac{dx_{\square e}}{dt} = -\kappa' x_{\square e} x_{\bigcirc B} \quad (45)$$

where $x_{\square A} \equiv x_{\square A}(t)$, $x_{\bigcirc B} \equiv x_{\bigcirc B}(t)$, and $x_{\bigcirc e} \equiv x_{\bigcirc e}(t)$ are, respectively, the number of unreacted □ groups on A blocks, the number of unreacted ○ groups on B blocks, and the number of unreacted □ groups on extender blocks, at time t ($x_{\square A}(0) = m_A n_A$, $x_{\bigcirc B}(0) = m_B n_B$, $x_{\square e}(0) = 2n_e$). In a stoichiometric system $x_{\square e} = x_{\bigcirc B} - x_{\square A}$ and, defining the degrees of reaction of species A, p_A, and chain extender, p_e, as

$$p_A = 1 - \frac{x_{\square A}(t)}{x_{\square A}(0)} \quad (46)$$

$$p_e = 1 - \frac{x_{\square e}(t)}{x_{\square e}(0)} \quad (47)$$

eqs 43 and 45 yield

$$\frac{dp_A}{dt} = \kappa(m_A f_A + m_B f_B)(1 - p_A)[\eta_A(1 - p_A) + \eta_e(1 - p_e)] \quad (48)$$

$$\frac{dp_e}{dt} = \kappa'(m_A f_A + m_B f_B)(1 - p_e)[\eta_A(1 - p_A) + \eta_e(1 - p_e)] \quad (49)$$

where we have absorbed a factor of $n_A + n_B$ into the definitions of the rate constants. The degree of reaction of species B is now readily obtained:

$$p = 1 - \frac{x_{\bigcirc B}(t)}{x_{\bigcirc B}(0)} = 1 - \frac{m_A f_A}{m_B f_B}(1 - p_A) - \left(1 - \frac{m_A f_A}{m_B f_B}\right)(1 - p_e) \quad (50)$$

This can be rewritten so as to display the stoichiometry more transparently:

$$(1 - \eta_A)p = \eta_A p_A + (1 - 2\eta_A)p_e \quad (51)$$

It is interesting to note that, from eqs 48 and 49, it follows straightforwardly that

$$(1 - p_A)^{\kappa'}(1 - p_e)^{\kappa} \quad (52)$$

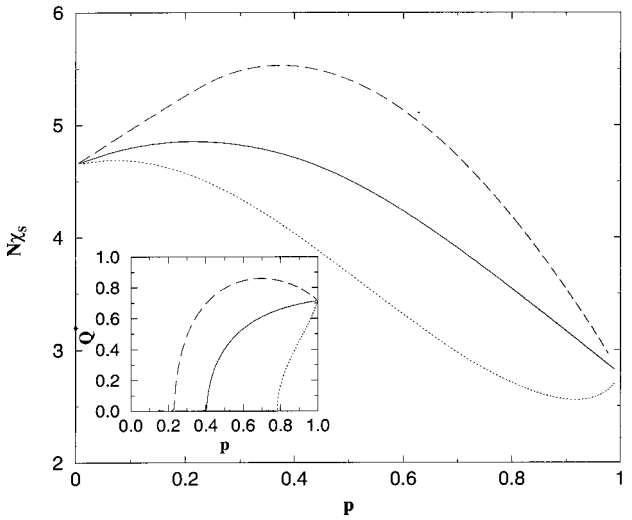

Figure 4. Spinodal as a function of p, the degree of conversion of B blocks, for $f_A = 0.2$, $\phi_A = 0.7$, and $b_B = 1$. $\kappa' = 1$ (solid line), 0.5 (dashed line), and 2 (dotted line). Inset: (Reduced) first unstable wavenumber, $Q^* = (Q_A^* Q_B^*)^{1/2}$, for the system in the main figure, with the same symbols as used there.

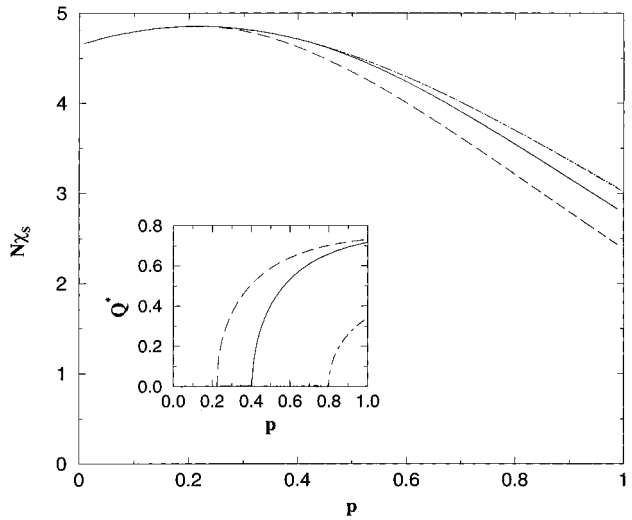

Figure 5. Spinodal as a function of p, the degree of conversion of B blocks, for $f_A = 0.2$ and $\phi_A = 0.7$. $\kappa' = 1$ and $b_B = 1$ (solid line), 0.5 (dashed line), 1.5 (dot−dashed line), and 2 (dotted line); the $b_B = 1.5$ and $b_B = 2$ curves are nearly indistinguishable. Inset: (Reduced) first unstable wavenumber, $Q^* = (Q_A^* Q_B^*)^{1/2}$, for the system in the main figure, with the same symbols as used there. Stiffening the polydisperse component (B) can completely suppress the tendency to microphase-separate. Notice the correlation between the appearance of a finite Q^* and the divergence of the spinodal curves for $b_B = 1$ and $b_B = 0.5$.

which serves as a check on any numerical method of solution. Note that, by eqs 50 and 52, p depends only on the *ratio* κ'/κ.

In the one-reaction-constant case, $\kappa = \kappa'$, eq 44 can be solved analytically, with the result

$$p = \frac{\kappa(m_A f_A + m_B f_B)\eta_B t}{1 + \kappa(m_A f_A + m_B f_B)\eta_B t} \tag{53}$$

In the foregoing we have assumed the reaction blend to be of spatially uniform composition, which of course will not be true, even approximately, beyond the very early stages of spinodal decomposition. Still, it is reasonable, as we are only looking for the instability of a *uniform* phase with respect to *infinitesimal* composition fluctuations.[38]

3. Results

Eqs 48 and 49 were solved for the degrees of reaction, p_A and p_e, using a fourth-order Runge−Kutta method with adaptive step size.[39] At each time t, eq 11 was solved by Brent's method.[39]

For greater generality we have chosen to present results for families of systems, characterized by certain ratios of their physical parameters. Each curve then refers to a whole such family, rather than an individual system. It follows from the definition of spinodal, eq 11, together with eq 5, and eqs 22−24 (for linear blocks) or 38−40 (for branched blocks) that χ_S is a function of N_α only through N; furthermore, it scales with $1/N$. Therefore $N\chi_S$ does not depend explicitly on block sizes (assuming, implicitly, that these are large enough for the theory to hold), and we plot it, along with the wave vector $\mathbf{q}^*$ for which the blend first becomes unstable on hitting the spinodal, as a function of p, the experimentally relevant quantity.[4,5,40] As remarked in the preceding section, p is a function of κ'/κ but not of the individual rate constants, and we can effectively measure time in units of κ^{-1}. Likewise, we take b_A as our unit of length, so henceforth a value of b_B will mean a ratio of Kuhn lengths b_B/b_A.

3.1. Linear A and B Blocks. All results are for a single composition, $f_A = 0.2$, $\phi_A = 0.7$. Figure 4 shows the spinodal for different κ'. It is seen that a faster A−B reaction ($\kappa' < 1$) enhances the stability of the mixed state, whereas a faster B-chain extender reaction ($\kappa' > 1$) favors demixing. This can be understood by realizing that the former case corresponds to the formation of more alternating sequences of A and B blocks within the chains (which are thus more diblock-copolymer-like in character and act as "compatibilizers"), whereas in the latter case there will be longer sequences of B blocks only (leading to a more homopolymer-like behavior: it is the increase in the degree of polymerization of B that drives phase separation).[7,8] One would then expect $\kappa' < 1$ to promote microphase separation, i.e., finite $\mathbf{q}^*$, and $\kappa' < 1$ bulk phase separation ($\mathbf{q}^* = 0$), which is indeed borne out by the calculation (see inset of Figure 4). Significantly, these effects are quite strong for a (realistic) factor of 2 difference in reaction rates. Note that all curves converge to the same limit when $p \to 1$, as the final state does not depend on the kinetics. In particular, the curve for $\kappa' > 1$ in Figure 4 exhibits a minimum at $p \lesssim 1$: all chain extender having been consumed, only the A−B reaction can proceed.

In Figure 5 the spinodal is plotted for $\kappa' = 1$ and different Kuhn lengths of the A and B blocks. Although a stiffer B block ($b_B > 1$) slightly stabilizes the mixed state, the impact is much less than that of different reaction constants. The nature of the instability, however, changes dramatically: a stiffer B block can suppress microphase separation completely in favor of bulk phase separation (see inset of Figure 5). Conversely, stiffer A blocks ($b_B < 1$) would sooner microphase-separate. In general, we have found that stiffening the longer block tends to favor microphase separation, i.e., if $N_A > N_B$ then making b_A larger will bias the system toward an instability at finite wave vector, whereas if $N_A < N_B$ the same will happen if b_B is made larger instead. Remarkably, the spinodal curves for $b_B \neq 1$ in Figure 5 only start to diverge from that for $b_B = 1$ at

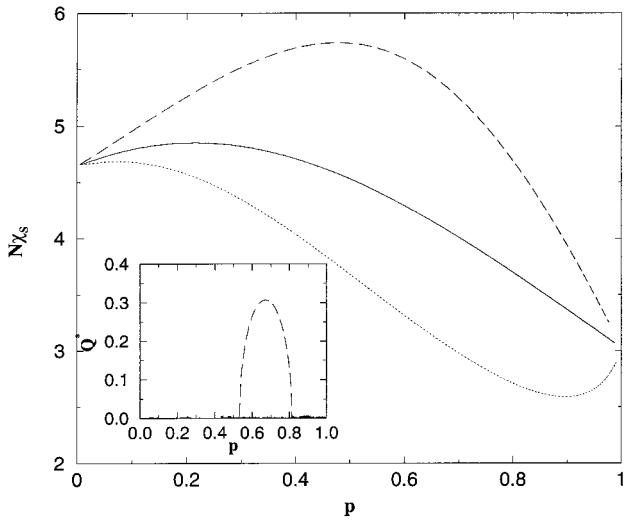

Figure 6. Spinodal as a function of p, the degree of conversion of B blocks, for $f_A = 0.2$ and $\phi_A = 0.7$. $b_B = 2$ and $\kappa' = 1$ (solid line), 0.5 (dashed line), and 2 (dotted line). Inset: (Reduced) first unstable wavenumber, $Q^* = (Q_A^* Q_B^*)^{1/2}$, for the system in the main figure, with the same symbols as used there. Note the remarkably "nonmonotonic" nature of the demixing instability: to microphase separation at intermediate degrees of conversion, but to bulk phase separation at both early and late times.

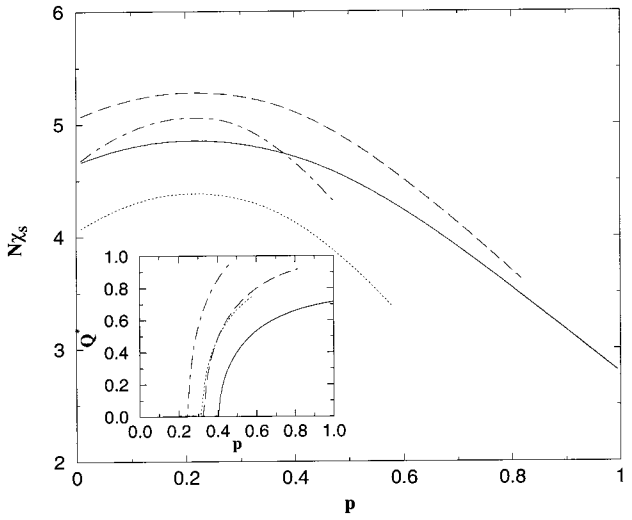

Figure 7. Spinodal as a function of p, the degree of conversion of B blocks, for $\eta_A = 0.2$, $\phi_A = 0.7$, $b_B = 1$, $\kappa' = 1$, and varying functionalities of the A and B blocks: $m_A = m_B = 2$ (solid line), $m_A = 4$, $m_B = 2$ (dashed line), $m_A = 2$, $m_B = 4$ (dotted line), and $m_A = m_B = 4$ (dot−dashed line). Inset: (Reduced) first unstable wavenumber, $Q^* = (Q_A^* Q_B^*)^{1/2}$, for the system in the main figure, with the same symbols as used there. Increasing the functionality of either block strengthens the tendency to microphase-separate, albeit for different reasons (see the text for details).

the Lifshitz points, i.e., when the first unstable wave vector becomes finite (see inset). This is because the Kuhn lengths only enter through the renormalized wave vectors $Q_\alpha \propto q$; see eqs 22−27.

The effect of combining different reaction rates and stiffnesses, belied by the apparent normality of the spinodals in Figure 6, is nevertheless dramatically displayed in the inset. Competition between the microphase-enhancing $\kappa' < 1$ (faster A−B reaction) and the microphase-suppressing $b_B > 1$ (greater stiffness of the polydisperse sections) conspires to produce a finite range of p where the blend first becomes unstable with respect to finite-wavelength fluctuations. Eventually, bulk phase separation wins, as the degree of polydispersity of pure B chain sections increases. Consequently, the resulting morphology is likely to be strongly dependent on the value of p at which the spinodal is crossed.

3.2. Branched A and B Blocks (Stars). As in the preceding subsection, all results are for a single composition, $\eta_A = 0.2$, $\phi_A = 0.7$. (f_A and f_B are no longer constant as m_A and/or m_B changes.) Each curve ends at the percolation threshold, beyond which the theory may not be meaningful, at least in the case of bulk phase separation. As expected, the higher the functionality, the earlier this threshold is reached; it also depends on the ratio of the reaction rates; see eqs 41 and 52.

In Figure 7 the functionalities of A and/or B blocks are varied, for equal reaction rates and Kuhn lengths. Varying m_A *or* m_B shifts the spinodal in opposite directions, but the absolute sense depends on composition: for the present choice of η_A and ϕ_A, larger m_A favors mixing and larger m_B demixing. As noted in ref 31, increasing m_A at constant block length N_A reduces the radius of gyration of the (monodisperse) A stars, yielding a blend with a stronger tendency to microphase-separate (see inset of Figure 7). The consequences of an increase in m_B are less straightforward to interpret. As B blocks become longer (see eq 20), microphase separation is again promoted, owing to the lower *effective* polydispersity of a branched object relative to a linear one:[41] the polydispersity is "spread more thinly over all arms". Put more formally: by the central limit theorem, the more B arms any "B cluster" is composed of, the narrower its size distribution will be.

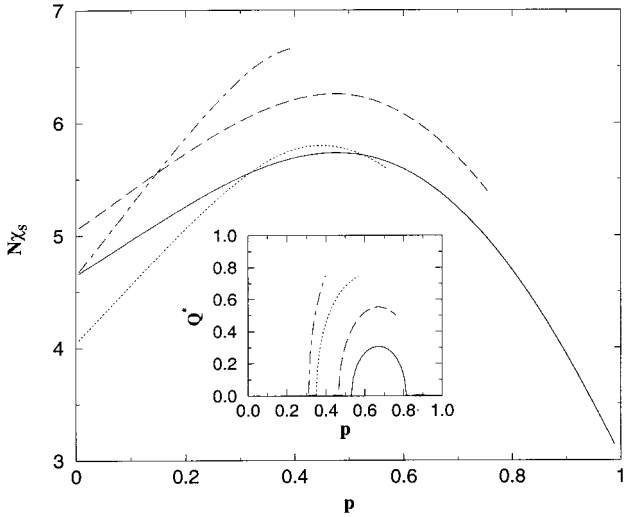

Figure 8. Spinodal as a function of p, the degree of conversion of B blocks, for $\eta_A = 0.2$, $\phi_A = 0.7$, $b_B = 2$, $\kappa' = 0.5$, and varying functionalities of the A and B blocks: $m_A = m_B = 2$ (solid line), $m_A = 4$, $m_B = 2$ (dashed line), $m_A = 2$, $m_B = 4$ (dotted line), and $m_A = m_B = 4$ (dot−dashed line). Inset: (Reduced) first unstable wavenumber, $Q^* = (Q_A^* Q_B^*)^{1/2}$, for the system in the main figure, with the same symbols as used there.

Figure 8 shows qualitatively the same effects, brought out more spectacularly by the choice of b_B and κ' that led to the dashed curves in Figure 6. Calculations performed for other values of κ' suggest that high degrees of branching alone do not seem to be able to create finite-wavelength instabilities where none previously existed (unless block B is made unrealistically short). Finally, by comparing the solid and dot−dashed curves, which correspond to $m_A = m_B$, and hence the

same N_A and N_B, we can conclude that "pure" higher functionality always stabilizes the blend and always predisposes toward microphase separation. This is true of all compositions investigated.

It should be emphasized that, by fixing the values of different parameters, we can obtain different "cuts" through the multidimensional composition space of the blend. In Figure 8, the solid and dashed (or dotted) curves on the one hand, and the solid and dot−dashed curves on the other, are examples of two such cuts.

4. Conclusions

We have extended the RPA treatment of a reacting binary polymer blend to account for different rates of the chemical reactions between the two polymer species and between one of them and a chain extender, as well as for different stiffnesses and functionalities of the two polymer chains. The richer and more realistic chemical kinetics thus introduced was found to have a substantial impact on the stability of the blend, as described by the liquid−liquid spinodal. The nature of the instability, i.e., whether it occurs with respect to bulk or microphase separation, is also affected. Moreover, the latter feature is particularly sensitive to changes in the relative molecular stiffness of the two polymers, which otherwise does not change the spinodal much. By simultaneously manipulating relative stiffnesses and reactivities, the fastest-growing unstable wave vector may be arranged to follow widely differing trajectories during the reaction. It is therefore possible to exercise considerable control over the morphology of the resulting system. Significantly, all these effects are seen for physically reasonable ratios of reaction constants and Kuhn lengths.

Work is in progress to extend the calculations presented here to other systems of practical importance, such as more complex polycondensation chemistries. Blends of more than two components can also be readily handled by increasing the dimensionality of the vectors and matrices.

References and Notes

(1) See, e.g.: *Encyclopedia of Polymer Science and Technology; Plastics, Resins, Rubbers*; Mark, H. F., Gaylord, N. G., Bikales, N. M., Eds.; Interscience: New York, 1964−1972.
(2) Doane, J. W. *MRS Bull.* **1991**, *16*, 22.
(3) For a discussion of TIPS and PIPS specifically in the context of PDLCs, see, e.g.: West, J. L. *Mol. Cryst. Liq. Cryst.* **1988**, *157*, 427.
(4) Elwell, M. J.; Mortimer, S.; Ryan, A. J. *Macromolecules* **1994**, *27*, 5428.
(5) Elwell, M. J.; Ryan, A. J.; Grünbauer, H. J. M.; Lieshout, H. C. V. *Macromolecules* **1996**, *29*, 2960.
(6) de Gennes, P. G. *Faraday Discuss. Chem. Soc.* **1979**, *68*, 206.
(7) Fredrickson, G. H.; Milner, S. T. *Phys. Rev. Lett.* **1991**, *67*, 835.
(8) Fredrickson, G. H.; Milner, S. T.; Leibler, L. *Macromolecules* **1992**, *25*, 6341.
(9) Shakhnovich, E. I.; Gutin, A. M. *J. Phys.* **1989**, *50*, 1843.
(10) Panyukov, S. V.; Kuchanov, S. I. *Sov. Phys. JETP* **1991**, *72*, 368.
(11) Panyukov, S. V.; Kuchanov, S. I. *J. Phys. II* **1992**, *2*, 1973.
(12) Dobrynin, A. V.; Erukhimovich, I. Ya. *JETP Lett.* **1993**, *57*, 125.
(13) Dobrynin, A. V.; Erukhimovich, I. Ya. *JETP* **1993**, *77*, 307.
(14) Dobrynin, A. V.; Erukhimovich, I. Ya. *Sov. Phys. JETP Lett.* **1991**, *53*, 570.
(15) Gutin, A. M.; Sfatos, C. D.; Shakhnovich, E. I. *J. Phys. A: Math. Gen.* **1994**, *27*, 7957.
(16) Dobrynin, A. V.; Erukhimovich, I. Ya. *J. Phys. I* **1995**, *5*, 365.
(17) Sfatos, C. D.; Gutin, A. M.; Shakhnovich, E. I. *Phys. Rev. E* **1995**, *51*, 4727.
(18) Dobrynin, A. V.; Leibler, L. *Europhys. Lett.* **1996**, *36*, 283.
(19) Panyukov, S. V.; Potemkin, I. I. *JETP Lett.* **1996**, *64*, 197.
(20) Dobrynin, A. V. *J. Chem. Phys.* **1997**, *107*, 9234.
(21) Dobrynin, A. V.; Leibler, L. *Macromolecules* **1997**, *30*, 4756.
(22) Angerman, H.; ten Brinke, G.; Erukhimovich, I. *Macromol. Symp.* **1996**, *112*, 199.
(23) Angerman, H.; ten Brinke, G.; Erukhimovich, I. *Macromolecules* **1996**, *29*, 3255.
(24) Angerman, H.; ten Brinke, G.; Erukhimovich, I. *Macromolecules* **1998**, *31*, 1958.
(25) Potemkin, I.; Panyukov, S. *Physica A* **1998**, *249*, 321.
(26) Potemkin, I. I.; Panyukov, S. V. *Phys. Rev. E* **1998**, *57*, 6902.
(27) Kuchanov, S. I.; Panyukov, S. V. *J. Polym. Sci. B* **1998**, *36*, 937.
(28) Slot, J. J. M.; Angerman, H. J.; ten Brinke, G. *J. Chem. Phys.* **1998**, *109*, 8677.
(29) Semenov, A. N. *J. Phys. II* **1997**, *7*, 1489.
(30) Semenov, A. N.; Likhtman, A. E. *Macromolecules* **1998**, *31*, 9058.
(31) Read, D. J. *Macromolecules* **1998**, *31*, 899.
(32) Edwards, S. F. *Proc. Phys. Soc.* **1966**, *88*, 265.
(33) de Gennes, P. G. *J. Phys.* **1970**, *31*, 235.
(34) Odian, G. *Principles of Polymerisation*; Wiley: New York, 1991.
(35) Shimada, T.; Doi, M.; Okano, K. *J. Chem. Phys.* **1988**, *88*, 2815.
(36) Clarke, N.; McLeish, T. C. B.; Jenkins, S. D. *Macromolecules* **1995**, *28*, 4650.
(37) de Gennes, P. G. *J. Phys.* **1977**, *38*, L-355.
(38) The effect of composition fluctuations on chain polymerization, and its impact on phase separation, has been examined by: Fredrickson, G. H.; Leibler, L. *Macromolecules* **1995**, *28*, 5198.
(39) Press: W. H.; Teukolsky, S. A.; Vetterling, W. T.; Flannery, B. P. *Numerical Recipes: The Art of Scientific Computing*, 2nd ed.; Cambridge University Press: Cambridge, 1992.
(40) Note that there is no symmetry under exchange of A and B, since B can follow B whereas A cannot follow A.
(41) Stockmayer, W. H. *J. Chem. Phys.* **1943**, *11*, 45.

MA990954D